

# Slip processes in the deformation of polystyrene

J. B. C. WU, J. C. M. LI

*Materials Science Program, and Department of Mechanical and Aerospace Sciences, University of Rochester, Rochester, New York, USA*

Two slip processes are characterized in the deformation of atactic polystyrene by compression. In the optical microscope, one appears as intensive shear bands and the other as diffuse shear zones. But in the electron microscope, the latter reveals itself in the form of two sets of numerous, fine, discontinuous shear bands intersecting at nearly right angles. In addition to their differences in appearance, the coarse slip band propagates fast along a localized path, inclines at less than  $45^\circ$  with the compression axis, and invariably produces shear fracture when it extends across the specimen. On the other hand, the fine slip bands spread slowly by multiplication mainly along the maximum shear stress direction, contribute to almost all the macroscopic strain and cause shape changes of the specimen. Hence the coarse band process is a brittle mode and the fine band process a ductile mode. The relative abundance of these bands depends on the thermal history of the specimen, the loading condition, and the deformation temperature. The average shear strain inside either band is about 1.5 and is recoverable upon annealing.

## 1. Introduction

Although yielding as a slip process has been well established in crystalline materials, it has only recently been studied in amorphous polymers. Whitney [1] seemed to be the first to report slip bands in polystyrene. Ender and Andrews [2] found similar bands in the delayed drawing of pre-oriented polystyrene. Argon *et al.* [3] studied the orientation of such bands originated in notched specimens. They found also that the slip bands are recoverable upon heating above the glass transition temperature. The entire shear strain of about 1 to 2 inside the slip band can be recovered. Bowden and Raha [4] investigated slip bands in both polystyrene and poly(methylmethacrylate) and found that, when the strain-rate decreases, slip bands gradually disappear and the deformation mode becomes diffuse with the appearance of "diffuse zones". They discovered also that slip bands are easier to form in annealed and slow-cooled specimens than quenched specimens. Brady and Yeh [5] studied the structure of slip bands and showed evidence of possible texture inside them. They found also that the slip bands

become less well defined with decreasing molecular weight. Bowden and Jukes [6] explained the orientation of slip bands in polystyrene by the classical plasticity theory. Kramer [7] made a Moiré analysis of the displacements around propagating slip band packets in polystyrene and found that these packets, although highly visible, contribute only a minor fraction to the total non-Hookean strain. The main contributors are the "diffuse shear zones" (same as "diffuse zones" mentioned by Bowden and Raha [4]). These "zones", unlike the slip bands, spread along the maximum shear stress directions ( $45^\circ$  to the compression axis).

These previous studies seem to indicate that there may be two deformation processes in polystyrene, one appears as slip bands and the other as diffuse shear zones. The former is much more localized than the latter. They respond differently to strain-rate and heat-treatment and behave differently in propagating direction and in their contribution to plastic strain. The fact that the shear zones spread along maximum shear stress directions indicates that it is also a slip process.

It is the purpose of this paper to study the microstructural differences of the two processes and that of the following paper to study their differences in yield behaviour.

## 2. Experimental

### 2.1. Sample preparation

The atactic polystyrene used in this study was obtained from the Westlake Co. in the form of 0.25 in. thick sheets. From gel permeation chromatography, the weight-average molecular weight was 599 000 and the number-average was 348 000. The glass transition temperature was 101°C determined by differential scanning calorimetry.

Blocks of the material cut from the sheet were annealed for 20 h at 115°C and either furnace cooled taking 5 h or quenched in air or liquid nitrogen. Samples were then cut from these blocks using a milling machine. Two shapes were used, 1 cm × 2 cm and 2 cm × 2 cm. A notch of 0.94 mm radius and 0.7 mm depth was cut out at the corner of some of the rectangular specimens. A hole of 1.2 mm diameter was drilled at the centre of some of the square specimens. All specimens were polished to 0.05 μm alumina finish. They were then annealed again at 95°C for 15 h to remove the residual stresses due to machining and polishing.

### 2.2. Replicas for electron microscopy

Polystyrene dissolves in most organic solvents, such as alcohol and benzene. Therefore, conventional two-stage replicating techniques using wax film, collodion, parlodion, etc. cannot be applied to polystyrene. Direct carbon replicas on bulk polystyrene cannot be obtained in the usual way because polystyrene swells when dissolving in solvents. A high resolution (resolvable to 25 Å) replicating technique based on Geil's method [8] with some necessary modifications was used. It is described step by step as follows:

(1) Shadow the specimen with Pt–C pallet wrapped with Pt–Pd wire (8 mil\* in diameter and 1 in. long). The shadowing angle is about 75° measured from the normal of the specimen surface to the straight line connecting the specimen and the evaporation source;

(2) Place a drop of 50% aqueous solution of polyacrylic acid at areas of interest on the shadowed surface and let dry for at least 6 h;

(3) Pick up the dried polyacrylic acid pieces.

\* 1 m = 3.9370 × 10<sup>4</sup> mil.

They should come off easily with the shadowing material tightly adhered;

(4) Evaporate a layer of carbon onto the Pd–Pt–C film which is now adhered to the polyacrylic acid;

(5) Dissolve the polyacrylic acid away in water using the filter paper method.

The results from the above technique should have very high resolution and high contrast provided that the surface of the specimen is well polished. When observing the diffuse zone, the specimen should be annealed after polishing. The annealing process causes surface diffusion which smooths out fine scratches from polishing and facilitates observations of very fine deformation features. These will be discussed later.

## 3. Results

### 3.1. The effects of strain-rate and cooling rate

A preliminary study shows that the slip bands will not appear without a stress concentration. Hence notched specimens were used for compression experiments. With the stress concentration, both the slip band and the diffuse zone can appear simultaneously as shown in Fig. 1. The effect of strain-rate is apparent confirming the findings of Bowden and Raha [4]. A more systematic study is shown in Fig. 2. Without the crossed polarizers, the diffuse zone cannot be seen and it is clear that the slip bands gradually disappear with decreasing

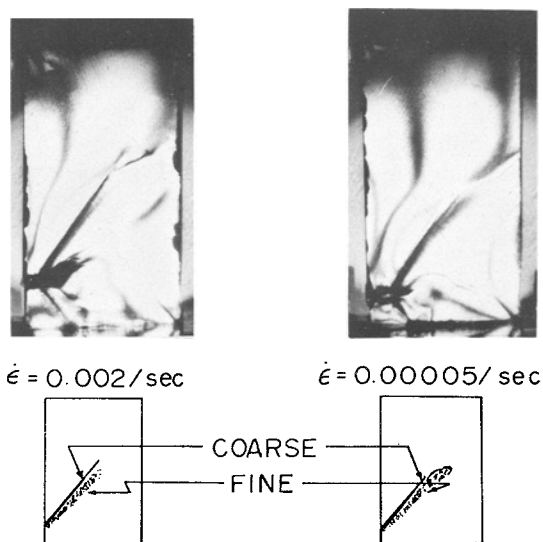


Figure 1 Slip bands and diffuse zones viewed between crossed polarizers.

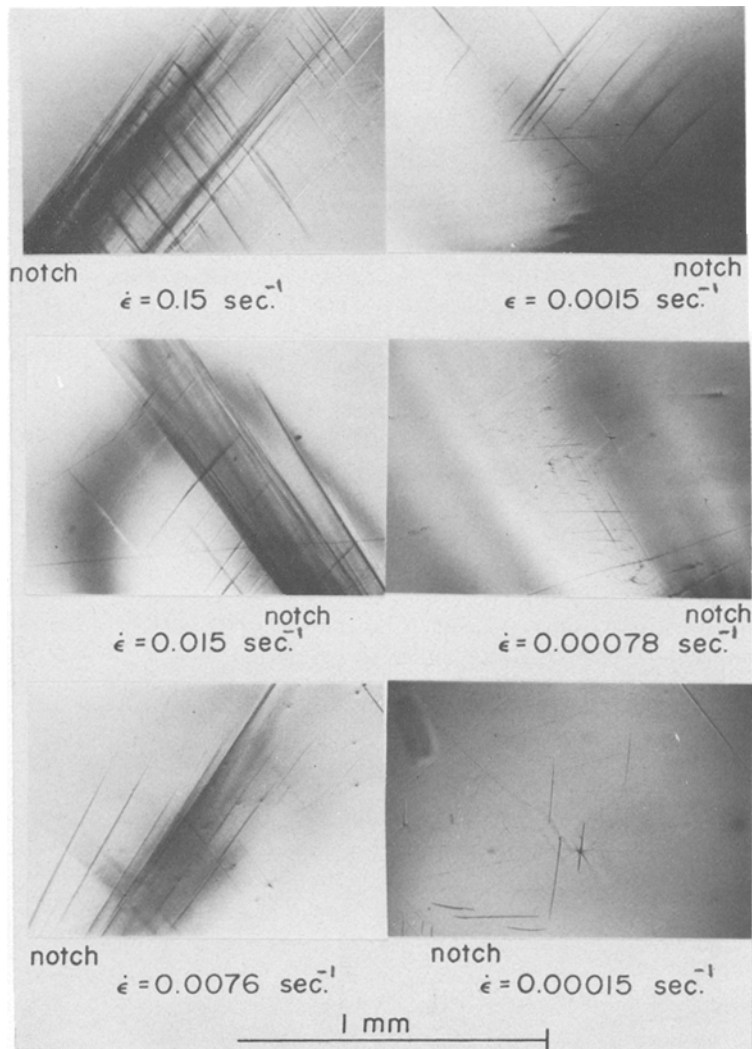


Figure 2 Strain-rate effect on the formation of slip bands.

strain-rate. Although the strain-rates were different, the pictures were taken for the same strain.

The effect of cooling is shown in Fig. 3. Two notched specimens, one furnace cooled and the other air cooled, were compressed at the same

strain-rate. It is clear that the furnace cooled specimens developed coarse slip bands while the air cooled specimens developed only the diffuse zones, confirming the findings of Bowden and Raha [4]. The diffuse zones appear merely as a

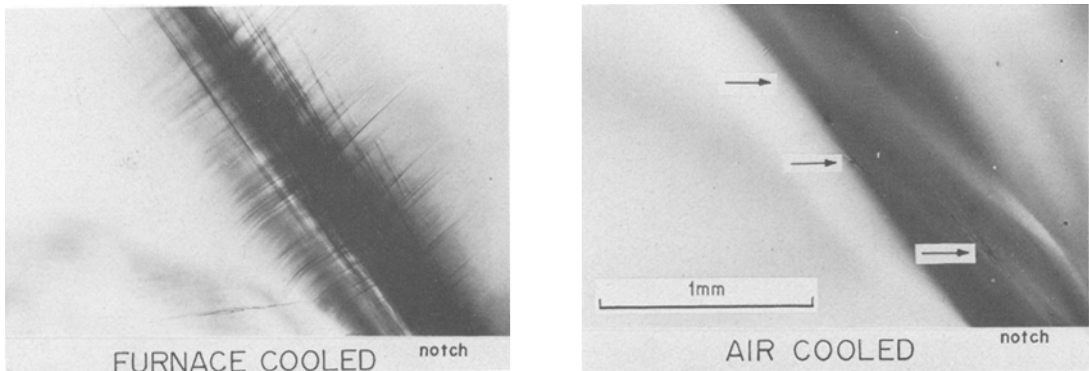


Figure 3 The effect of cooling on the formation of slip bands.

bulge in the photograph. The arrows point to some stress concentrators which seem to serve as sources for the initiation of the diffuse zones. This effect of cooling enables us to study the characteristics of slip bands and diffuse zones separately without interfering with each other.

### 3.2. The diffuse zone under high magnification

At higher magnification with Nomarski contrast the difference in appearance between the slip band and the diffuse zone is shown more clearly in Fig. 4. The diffuse zone appears to consist of very fine bands. In order to examine these fine bands more closely, replicas were made for observation in the electron microscope. The procedures for making replicas have been described in the Experimental section. A region with both the slip bands and the diffuse zone is shown in Fig. 5. It is seen that the thin bands in the diffuse

zone are extremely fine and they are not as localized and continuous as the coarse slip bands which are seen also in Fig. 5. These latter are not only much more well defined but also inclined at a different angle. Because of the new look of the diffuse zones, they will be renamed “fine slip bands” so as to differentiate from the “coarse bands” which can be seen clearly in the optical microscope.

In the literature [3, 4] the “diffuse zone” has been referred to as homogeneous deformation; its new look suggests that the deformation is still inhomogeneous in the diffuse zone. Since both the “coarse bands” and the “fine bands” are inhomogeneous deformation, it is very likely that they represent two distinctly different slip processes. Such differences do not imply that they are independent of each other. In fact each is seen in Fig. 5 to be convertible into the other during deformation.

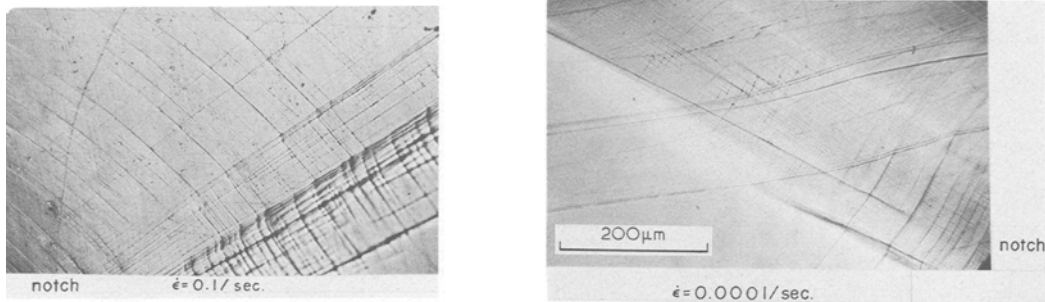


Figure 4 Coarse and fine slip bands under optical microscope with Nomarski contrast.

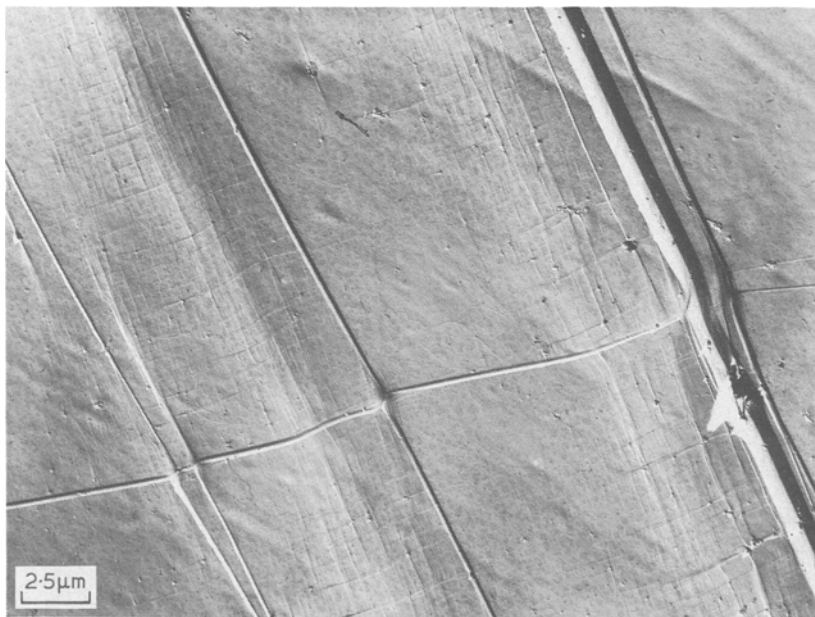


Figure 5 Coarse and fine slip bands in polystyrene.

### 3.3. Evidence for slip and shear

As shown in Fig. 6, the slip bands invariably displace all the scratches on the surface similar to the slip bands in crystalline materials. The shear strain can be calculated by the displacement of the scratch divided by the thickness of the slip band. The results of at least 20 measurements on slip bands with various thicknesses

indicate that the shear strains are between 1.2 and 1.6. Fig. 7 shows another interesting result. The specimen was compressed at a very high strain-rate ( $0.5 \text{ sec}^{-1}$ ) and was fortunately stopped in time before fracture occurs. A visible wide band was formed from the notch to the other end of the specimen. The shear strains measured along the entire band fall between 1.2 and 1.6. Such

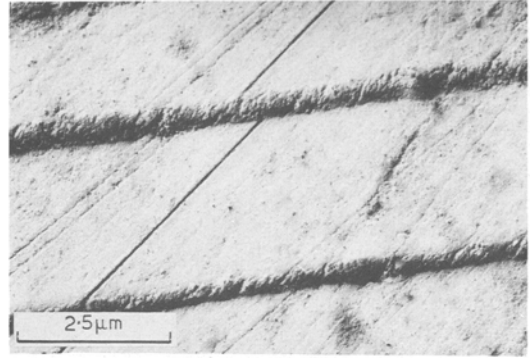
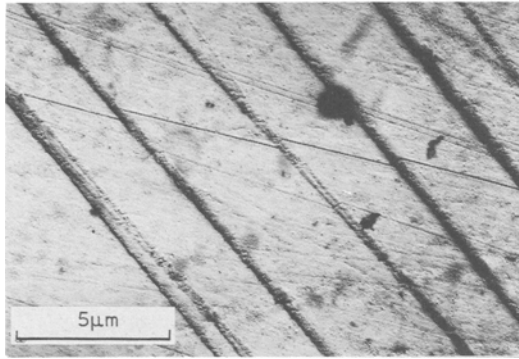


Figure 6 Scratches displaced by coarse slip bands.

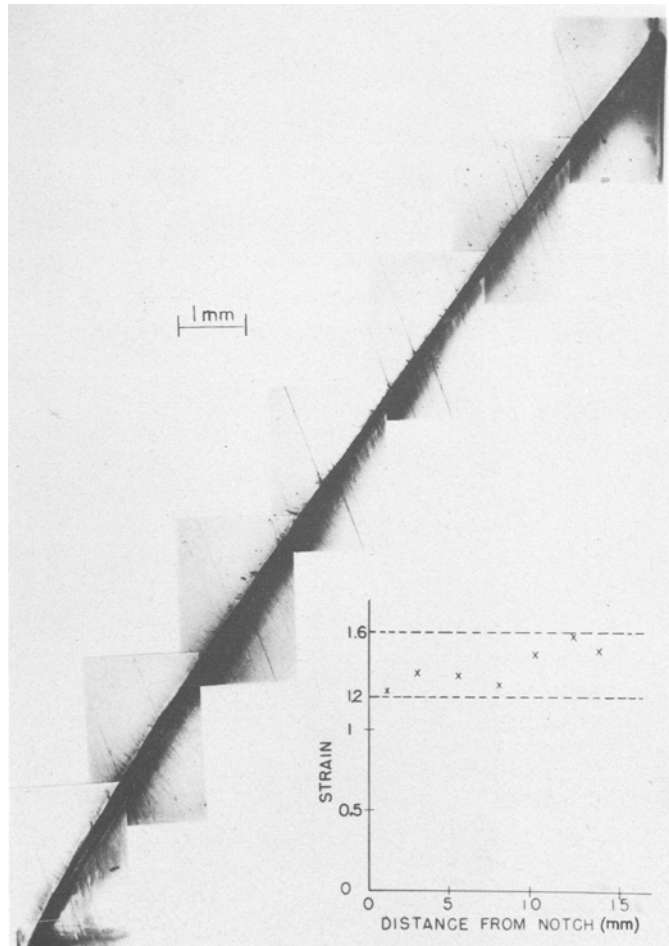


Figure 7 Shear strain along a long coarse slip band.

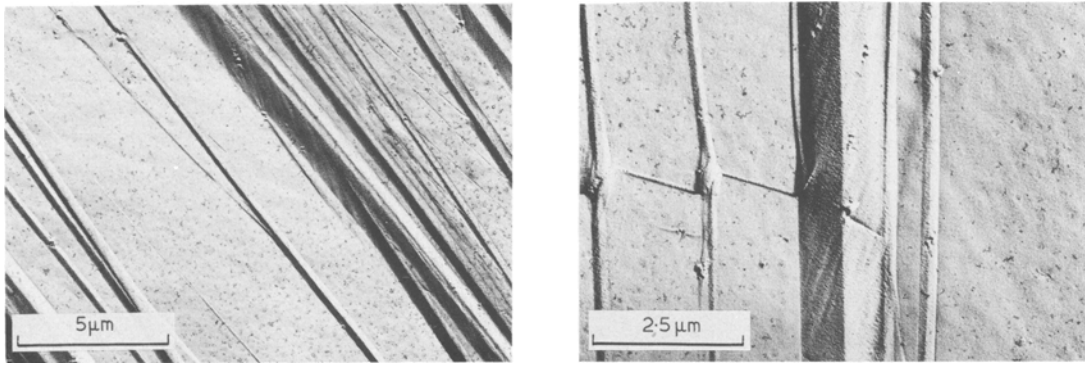


Figure 8 Electron micrograph of the morphology of coarse slip bands.

magnitude of strain must be an intrinsic property of the molecular process involved in the formation of the slip bands.

Argon *et al.* [3] first reported that the shear strains within the slip bands are between 1 and 2.15 obtained by the same technique. Because they did not report the observation of any splitting of the slip bands, their lower margin may be an underestimate. Bowden and Raha [4] obtained the value 2 (later corrected by Bowden [9]) in shear strain by measuring the angle between the optical extinction direction and the slip band direction. The angle was found to be between  $20^\circ$  and  $23^\circ$ . As shown in Fig. 8, there are parallel striations inside the slip band making an angle about  $21^\circ$  with the same. Several such angles were measured. They all fall between  $18^\circ$  and  $23^\circ$ . Thus it is quite possible that these striations are the cause of optical extinction since the angles are close to what Bowden and Raha measured.

### 3.4. Morphology of slip bands

There are two sets of coarse bands intersecting at an angle other than  $90^\circ$  as shown in Fig. 5. In areas away from the notch, the set starting from

the notch has more and wider bands than the other set. Near the notch, however, they are equally abundant. At very high strain-rates, the slip bands starting from the notch form a visible packet and propagate to the other side of the specimen, while the other set of slip bands can only be barely seen near the notch.

From the electron micrographs shown in Fig. 8, it can be seen that the thickness of coarse bands varies from 300 to 19 000 Å (30 to 1900 nm). In some places, cross-slip appears as a splitting of the slip band. Such cross-slip could result from local stress inhomogeneities in the specimen. The black and white contrast in each band indicates a bulge on the surface, which seems proportional to the thickness of the band. Such dimensional change of the deformed region has not been reported before. It seems to indicate that each band no longer consists of even finer bands. When the band thickens, the additional slip is probably not limited to the undeformed region but rather throughout the whole band. It may even indicate that the shear strain is not uniform within the band but is largest in the middle.

It was stated by Argon *et al.* [3], and also by

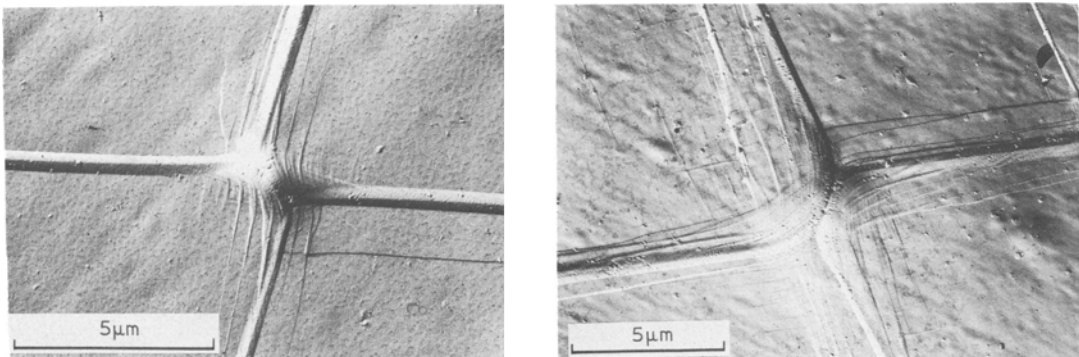


Figure 9 Electron micrograph of the intersection of coarse slip bands.

Brady and Yeh [5], that once a slip band (coarse) forms and attains a certain thickness it grows only in length. The present observation on the intersections of coarse slip bands suggests that the slip bands do grow in thickness as well as in length. As shown in Fig. 9 the intersecting slip bands are sheared by each other. Unless they meet at the same time, which is unlikely because every intersection observed shows that both bands are sheared, the only possible mechanism is that both slip bands grow in thickness during deformation to produce the observed shearing.

Another observation that is worth mentioning is the “nodular” structure within the slip band reported by Brady and Yeh [5]. The specimens used in Figs. 5 and 8 were annealed after polishing. The slip bands show the striations, not the nodular structure observed by Brady and Yeh [5]. However, in Fig. 6, where the specimen used was not annealed after polishing, the nodular structure appears inside the slip bands. Therefore, the nodular structure reported is likely the result of surface defects which are introduced by mechanical polishing.

As discussed earlier, the fine slip bands are abundant at low strain-rates. Fig. 10 shows another electron micrograph of the fine slip bands.

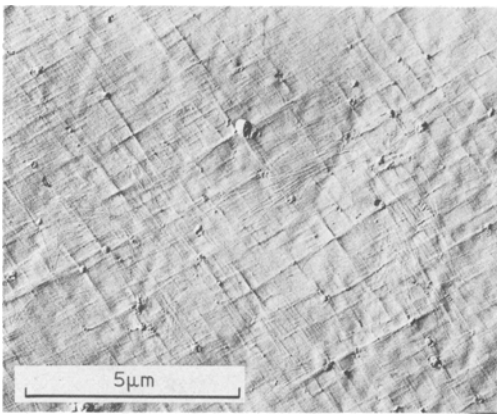
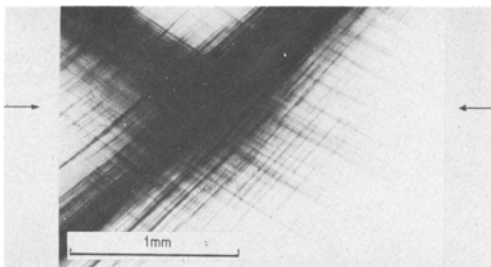


Figure 10 Electron micrograph of fine slip bands.



They seem to initiate at some local defects and then become diffuse as they propagate away from the place of initiation. Most of these defects are usually very small in size. Some abnormally large defects can be seen in a low magnification optical micrograph, such as those indicated by arrows in Fig. 3. These defects have not been characterized.

### 3.5. Craze formation at slip band intersections

The intersection of two slip bands is of interest. As pointed out by Hull [10] such intersection could be important in the fracture process, since it is conceivable that crazes and cracks may start from these intersections. Fig. 11 shows such craze formation at the intersection of coarse slip bands. It is noted that the craze plane is approximately perpendicular to the compression axis. This fact clearly indicates that the craze was caused by the local stress field of slip bands since otherwise it should not be formed under compressive loading.

The intersection of fine slip bands is also capable of craze formation. Unlike the coarse slip bands, the crazes caused by the fine slip bands are in two directions, as shown in the right lower photograph of Fig. 2. Those perpendicular to the compression axis were formed after the release of load and those parallel were formed during loading.

It is known that craze formation requires tensile stress [11]. During compression, the tensile stresses can be caused by the slip bands as illustrated in Fig. 12 using a dislocation model. It should be noted that these dislocations are Volterra dislocations [12]. When the specimen is in compression, a tensile stress perpendicular to the compression axis may not be developed to its full extent. After the load is removed, the tensile stress then may be sufficient to produce crazes perpendicular to the compression axis.

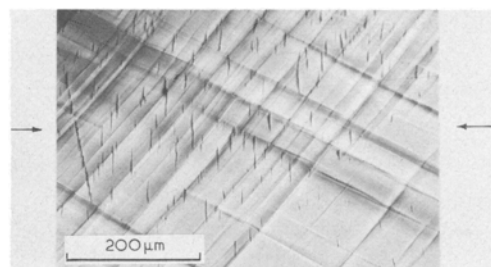


Figure 11 Craze formation at the intersection of coarse slip bands.

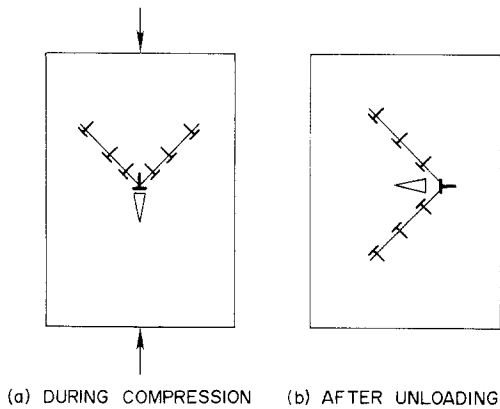


Figure 12 Craze formation by slip bands.

The reason why the coarse slip bands do not induce crazes parallel to the compression axis is probably due to the fact that crazing is a much slower process than the formation of coarse slip bands. Crazes parallel to the compression axis may not have enough time to initiate.

### 3.6. Chemical etching of slip bands

It is known that the coarse slip bands can be etched by strong oxidizing agents [13]. A deformed specimen was immersed in the mixture of chromic and sulphuric acids (50-50) at 90°C for ½h. The result is shown in Fig. 13. It is seen that not only the coarse slip bands can be etched, but also the fine slip bands. The coarse bands show a line-up of etch pits and the fine slip bands show a conglomerate of random etch pits. The fact that the fine slip bands can be etched is very helpful in determining the yielding criterion, which will be discussed in the subsequent paper. Although it is clear that the etch pits are related to the slip bands, the process involved in their formation is not yet known. However, from the

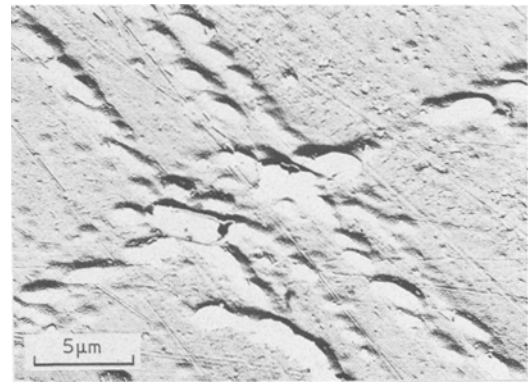
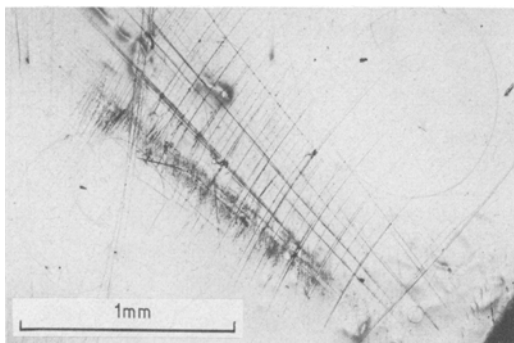


Figure 14 Electron micrograph of etch pits of coarse slip bands.

electron micrographs of the replicas of etch pits, such as the one shown in Fig. 14, the etch pits in the coarse bands may show a direction related to the striations mentioned earlier.

### 3.7. Recovery of slip bands

Argon *et al.* [3] reported that the coarse slip bands in polystyrene can be recovered by heating the specimen above the glass transition temperature. Haward *et al.* [14] also observed the recovery of a broad shear band (fine slip bands) after annealing the specimen above  $T_g$ . In this study, it is found that the recovery also takes place below  $T_g$ , although the time required is very long. As an example, at 88°C, a coarse band with a displacement of 29µm at a scratch reduced to 25µm or 14% recovery after annealing for 20 h. In another specimen annealed at  $T_g$  (101°C) for 4 h, a displacement of 15 µm was fully recovered.

An experiment was designed to observe the morphology of slip bands on the recovered specimens. When the slip bands recover, they generally do not leave traces, especially the fine slip bands. Therefore, a decoration technique was

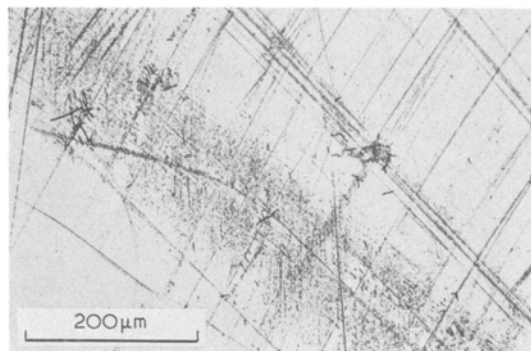
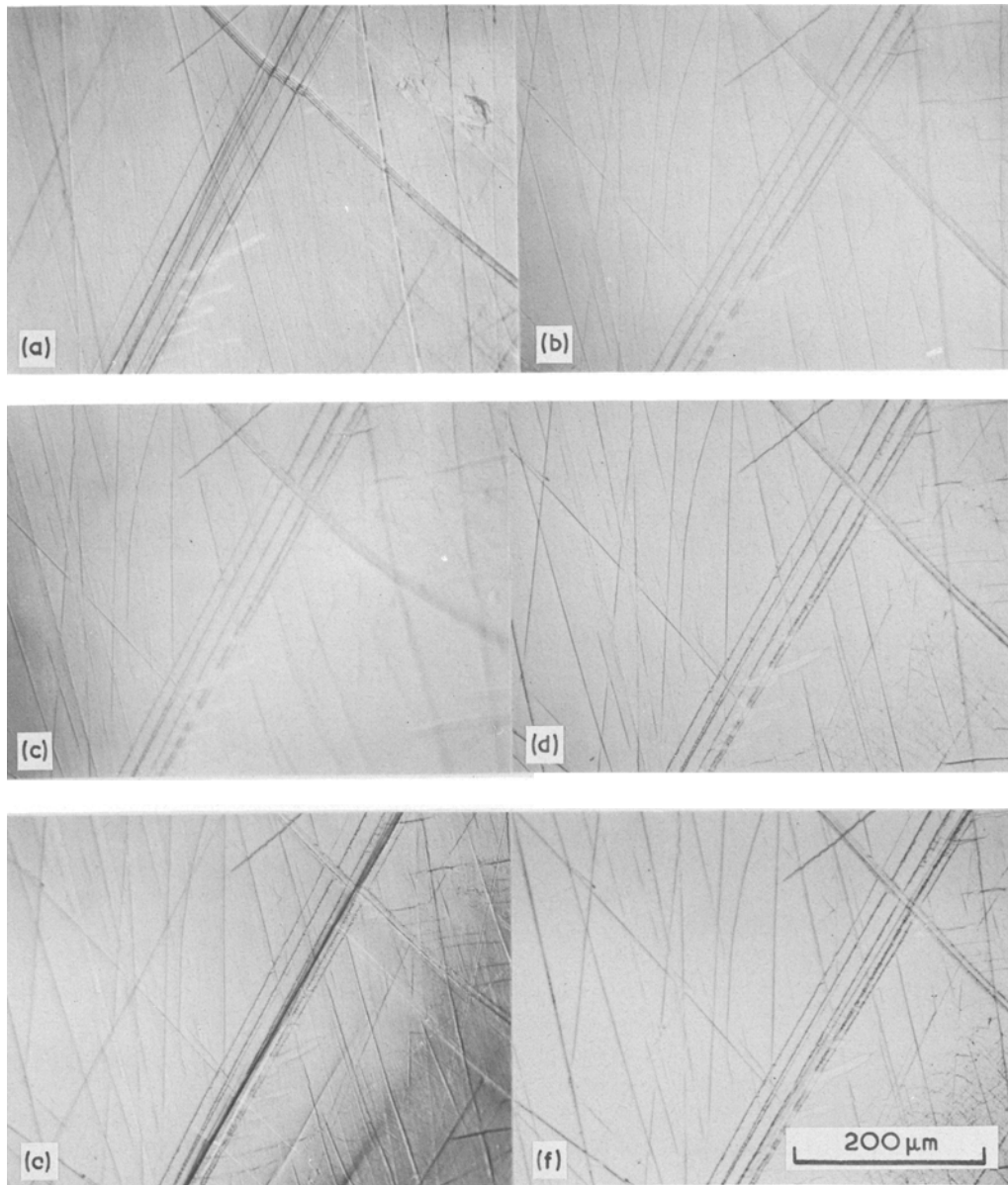


Figure 13 Etch pits of slip bands.





*Figure 15* Recovery and re-initiation of slip bands.

used. The banded surface was first coated with a thin layer of gold by vapour deposition in vacuum. After annealing, the gold film collapses at the locations of the slip bands, thereby leaving the traces of the recovered slip bands.

Using this technique, it is found that cooling from the annealing temperature still plays an important role in the formation of the slip bands in the recovered specimens. Fig. 15 shows a sequence of photographs of alternate compression and annealing. The strain-rate used was  $5 \times 10^{-3} \text{ sec}^{-1}$ . Fig. 15a shows a packet of coarse slip bands, which can be identified by the shearing

of the scratches. After annealing at  $115^\circ\text{C}$  for 30 min, the decorated coarse slip bands are shown in Fig. 15b. The recovery is evident by the straightening out of the scratches. The specimen was then air-cooled and compressed again at the same strain-rate to the same strain. Fig. 15c shows the same area of re-compressed specimen. No shearing of scratches can be observed. Instead, the presence of fine slip bands can be seen by the bending of the big scratch that runs perpendicular to the slip bands. These fine slip bands get decorated after annealing at  $115^\circ\text{C}$  for 30 m, which is shown in Fig. 15d. Again, the scratches are straight-

ened out. The specimen was furnace-cooled after annealing and compressed at the same strain-rate again. The appearance of a coarse slip band is seen in Fig. 15e by the displacement of the scratch. Another annealing recovered the displacement as shown in Fig. 15f.

It is interesting to note that the recovered coarse slip bands do not operate again during re-compression. Fig. 16 shows a better view. The new bands can be distinguished from the old trace by their solid continuous appearance. It can be seen that the scratches are displaced by the new bands and not by the old trace. However, the stress-strain curve of the specimen is found not

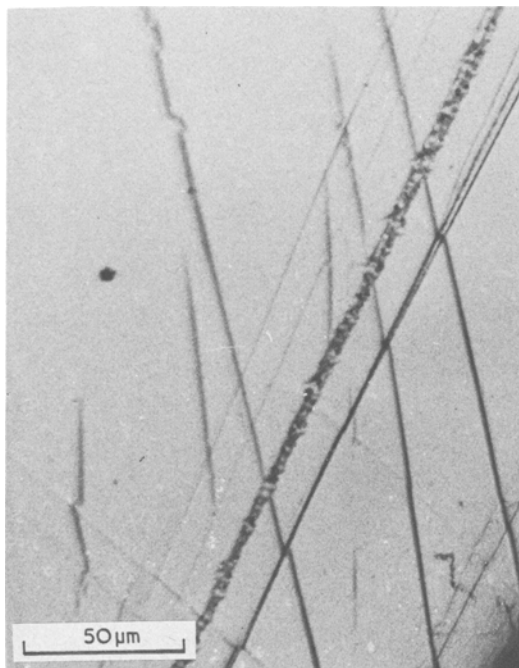


Figure 16 Newly formed coarse band and trace of recovered coarse band.

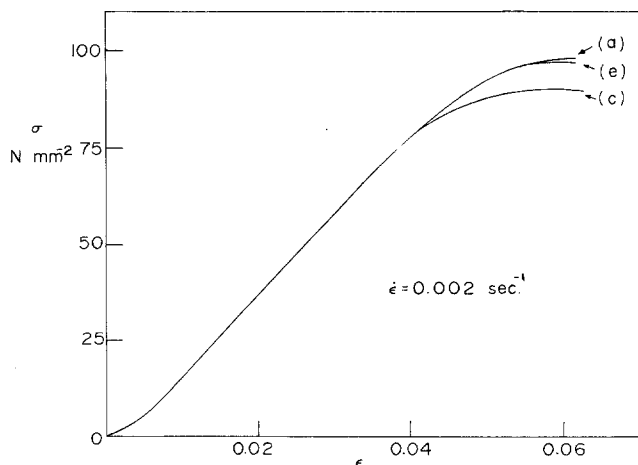


Figure 17 True stress-true strain relations for the specimen in Fig. 15.

affected significantly by the recovery annealing. As shown in Fig. 17 the stress-strain curves of the specimens used in Fig. 15 are compared. Air-cooling can lower the maximum stress about  $8 \text{ N mm}^{-2}$  without changing Young's modulus. The recovered specimen, if furnace cooled, has about the same stress-strain curve as the original.

### 3.8. Ductility of slip bands

The coarse slip band packets, in general, induce shear fracture when they reach the other side of the specimen. The plastic strain is small. So the coarse slip process is a brittle mode. On the other hand, when a fine slip band packet reaches the other side of the specimen, it produces a large kink. Further deformation can cause tensile fracture by initiating and expanding crazes parallel to the compression axis. The fine slip process is a ductile mode since it fractures the specimen only after large plastic strains. These differences are shown in Fig. 18.

## 4. Summary and conclusions

(1) Two slip processes during the compression of atactic polystyrene are characterized. One appears as coarse slip bands in the optical microscope and the other as fine slip bands in the electron microscope by using a high resolution replicating technique.

(2) The coarse slip bands appear in high speed deformation and the fine slip bands appear in low speed deformation.

(3) Furnace cooled specimens develop coarse slip bands and air cooled specimens develop fine slip bands.

(4) The coarse slip bands displace all scratches on the surface and the average shear strain is about



Figure 18 Difference in ductility of coarse and fine slip bands.

1.2 to 1.6 inside the band. On the mechanically polished surfaces without annealing, the coarse slip bands show “nodular” structure inside them. By annealing after polishing, the coarse bands show striations and a well defined bulge over the surface. The striations make an angle of  $18^\circ$  to  $23^\circ$  with the band direction.

(5) Both slip bands thicken during deformation and shear each other at intersections.

(6) Crazes appear at the intersection of both coarse and fine slip bands, some during loading and others after unloading. A dislocation model is proposed for the source of internal stresses.

(7) Both slip bands develop etch pits on the surface when immersed in 50-50 mixture of chromic and sulphuric acids at  $90^\circ\text{C}$  for  $\frac{1}{2}$  h.

(8) Both slip bands recover their shear strains upon annealing. A gold decoration technique is useful to reveal the recovered bands. Reloading after annealing does not activate recovered coarse bands. New bands are nucleated instead. The reloading stress-strain curve is about the same as before annealing.

(9) Coarse slip bands cause brittle fracture after they extend across the specimen. Fine slip bands cause ductile fracture after large strains. Thus the former is a brittle mode and the latter a ductile mode.

### Acknowledgements

The molecular weights and the glass transition temperature for the polystyrene used were kindly determined for us by S.E.B. Petrie and A.L.

Spatorico of Eastman Kodak Co. This research was partially supported by the Army Research Office, Durham, North Carolina through contract DA-ARO-D-31-124-73-G77.

### References

1. W. WHITNEY, *J. Appl. Phys.* **34** (1965) 3653.
2. D. H. ENDER and R. D. ANDREWS, *ibid* **36** (1965) 3057.
3. A. S. ARGON, R. D. ANDREWS, J. A. GODRICK and W. WHITNEY, *ibid* **39** (1968) 1899.
4. P. B. BOWDEN and S. RAHA, *Phil. Mag.* **22** (1970) 463.
5. T. E. BRADY and G. S. Y. YEH, *J. Appl. Phys.* **42** (1971) 4622; *J. Mater. Sci.* **8** (1973) 1083.
6. P. B. BOWDEN and J. A. JUKES, *J. Mater. Sci.* **7** (1972) 52.
7. E. J. KRAMER, *J. Macrom. Sci.-Phys.* **B10** (1974) 191.
8. P. H. GEIL, “Polymer Single Crystals, Polymer Reviews”, Vol. 5 (Interscience, New York, 1963).
9. P. B. BOWDEN, in “The Physics of Glassy Polymers” (edited by R. N. Haward) (Wiley, New York, 1973) p. 279.
10. D. HULL, in “Polymeric Materials, Relationship bet. Structure and Mechanical Behavior”, ASM Seminar, 1973 (ASM, 1975).
11. S. S. STERNSTEIN, L. ONGCHIN and A. SILVERMAN, *Appl. Polymer Symp.* **7** (1968) 175.
12. J. C. M. LI and J. J. GILMAN, in “Polymeric Materials, Relationship bet. Structure and Mechanical Behavior”, ASM Seminar, 1973 (ASM 1975) p. 239.
13. J. C. M. LI, C. A. PAMPILLO and L. A. DAVIS, “Deformation and Fracture of High Polymers” (edited by H. H. Kausch, J. A. Hassell and R. I. Jaffee) (Plenum Press, New York, 1972) p. 239.
14. R. N. HAWARD, B. M. MURPHY and E. F. T. WHITE, *J. Polymer Sci. A-2* **9** (1971) 801.

Received 9 July and accepted 29 July 1975.